

Original Article

# Automated Brain Tumour Detection and Classification Using Equilibrium Optimization Algorithm with Deep Learning Model

A. Asma Parveen<sup>1</sup>, T. Kamalakannan<sup>2</sup>

<sup>1</sup>School of Computing Science, VISTAS: Vels Institute of Science Technology & Advanced Studies, Tamilnadu, India.

<sup>2</sup>Department of Information Technology (BCA & IT), School of Computing Sciences, VISTAS: Vels Institute of Science Technology & Advanced Studies, Tamilnadu, India.

<sup>1</sup>Corresponding Author : [asmaparveenresearchscholar@gmail.com](mailto:asmaparveenresearchscholar@gmail.com)

Received: 12 October 2023

Revised: 23 November 2023

Accepted: 14 December 2023

Published: 23 December 2023

**Abstract** - Earlier diagnosis and classification of Brain Tumour (BT) with high prognosis accuracy is the most crucial step for detection and treatment to increase the survival rate of the patient. However, the manual inspection of brain MR images is time-consuming for doctors and radiologists to localize and identify cancer and normal tissues and classify the tumours from clinical imaging datasets. A Computer-Aided Diagnosis (CADx) technique is paramount to address these problems. It must be implemented to facilitate radiologists or doctors and relieve the workload in medical imaging analysis. Lately, researcher workers have introduced accurate and robust solutions to automate the detection and classification of BT. Classical Machine Learning (ML) techniques were exploited for the analysis of BT. Deep Learning (DL) has combined feature extraction and classification into a self-learning method on a large number of labelled datasets, which dramatically improves the performance. Therefore, the study presents an Automated BT Detection and Classification technique on MRIs using Equilibrium Optimization with Deep Learning (ABTDC-EODL). The goal of the ABTDC-EODL approach is to classify BT among adults as well as kids under the age of 10. Primarily, the ABTDC-EODL technique involves a Wiener Filtering (WF) technique to discard the noise that exists in it. To derive features, the ABTDC-EODL technique uses the ShuffleNet model, and the EO algorithm can choose its hyperparameters. Finally, the Stacked Autoencoder (SAE) model was utilized to identify the presence of BT. The ABTDC-EODL model can be validated on a benchmark Br35H: Brain Tumour Detection 2020 dataset, which encompasses 1500 tumorous and 1500 non-tumorous images. The obtained values highlight the better results of the ABTDC-EODL algorithm over other existing techniques.

**Keywords** - Brain Tumour, Equilibrium optimizer, Computer Aided Diagnosis, Deep Learning, MRI.

## 1. Introduction

A Brain Tumour (BT) is a large number of abnormal cells that develop in the inflexible skull surrounding the brain. Some developments within this limited region can give rise to problems [1]. Some kinds of cancer growing inside the skull lead to brain damage that poses a significant risk to the brain. BTs rank as the tenth most common cause of mortality in both children and adults [2]. Several diverse types of cancer, and everyone has low survival rates depending on the shape, location, and texture.

Recently, various imaging methods have been developed that not only demonstrate the comprehensive and whole aspects of BTs but also support physicians in accurately analyzing the cancer and deciding the right treatment techniques. MRI is regarded as the most famous imaging approach to identifying BTs [3]. There is no exposure of the

patients to extreme ionization radiation. MRI has an excellent and non-excellent soft tissue contrast imaging process, which provides crucial data about BT size, location, and shape [4]. The BT analysis was extremely time-intensive and hugely dependent upon the radiologist's knowledge and experiences. Due to there being more patients, the quantity of information that can be processed is substantially developed, making standard methods inaccurate and expensive.

The problems are related to significant BT intensity variations, shape, and size for similar types of cancer and the same appearances of other categories of disease [5]. A misclassification of a BT may lead to severe effects and decrease the patient's survival rate. There is increased attention to making automatic technologies for image processing to address the drawbacks of manual diagnoses and other relevant applications [6]. Numerous systems for



Computer-Aided Diagnosis (CAD) have been developed to detect BTs automatically. The latest achievements in Machine Learning (ML), especially in DL, have resulted in the classification and diagnosis of medical imaging patterns [7]. Accomplishments in this field comprise the probability of recovering and removing information from data rather than learning from medical specialists or scientific texts [8]. ML has quickly become a supportive tool to enhance effectiveness in different medical applications in different fields, comprising the analysis and prognosis of diseases, detection of cellular and molecular structures, tissue segmentation, and image classification.

In image processing, the most effective methods presently employed are Convolutional Neural Networks (CNNs), as they have several layers and higher diagnostic reliability when the quantity of input images is higher [9]. Autoencoders (AE) have been an unsupervised learning technique that neural networks were leveraged for representation learning. Particularly, different DL and ML methods are employed for detecting cancers like lung cancer and identifying cardiovascular stenosis. Additionally, performance estimations are indicated that can be a higher accuracy of diagnosis [10]. Several research studies have been carried out on the identification of BTs by diverse models and techniques. This article introduces an Automated Brain Tumour Detection and Classification technique on MRIs using Equilibrium Optimization with Deep Learning (ABTDC-EODL).

The goal of the ABTDC-EODL approach is to classify BT among adults as well as kids under the age of 10. Primarily, the ABTDC-EODL technique involves the Wiener Filtering (WF) technique to discard the noise that exists in it. To derive features, the ABTDC-EODL technique uses the ShuffleNet model and its hyperparameters are selected by the EO technique. Finally, the Stacked Autoencoder (SAE) model was utilized to identify the presence of BT. The ABTDC-EODL model can be validated on a benchmark Br35H: Brain Tumour Detection 2020 dataset, which encompasses 1500 tumorous and 1500 non-tumorous images.

## 2. Related Works

Ruba et al. [11] developed a CNN model that can be two subnetworks, namely Local Symmetry Inter Sign (LSIS) based Intra Tumour Segmentation Network (LITSN) and Tumour Localization Network (TLN). In TLN, 3DUNet could be employed for localizing the tumour. Subsequently, intra-cancer areas are segmented utilizing Deep-CNN (DCNN), which presents a new technique that can depend on LSIS.

In [12], a DL and standard ML algorithm were combined for the detection of BT. ResNet-18 and AlexNet have been exploited with the SVM approach for analysing and classifying BT. Diagnostics of BT utilizing MRI images were

improved through the average filter algorithm. Next, DL methods have been implemented for extracting robust and significant deep features by deep convolutional layers. Toğaçar et al. [13] implemented a CNN approach termed as BrainMRNet. Primarily, after pre-processing, this stage is transmitted to attention mechanisms employing image augmentation methods for all images.

Attention mechanisms choose significant image fields, and the image is transmitted to convolutional layers that employ hypercolumns. Applying this, the feature extraction from all layers of the BrainMRNet system was maintained by the array structure in the final layer. In [14], a novel hybrid technique that integrates the PSO method with CNNs for improving classification and identification abilities was introduced. This technique employs the PSO method to find the optimum structure of CNN hyper-parameters. Then, enhanced parameters have been implemented in the CNN models for classification. Arif et al. [15] introduced a diagnosis and segmentation technique for BTs.

This developed technique is studied and is dependent upon Berkeley's Wavelet Transformation (BWT) and DL method for increasing effectiveness as well as simplifying the techniques of medical imaging segmentation. Important features must be removed from every segmented tissue utilizing a Gray-Level-Co-occurrence Matrix (GLCM) approach and then a feature optimization applying GA. In [16], a DL approach for the segmentation of BTs was introduced. A CNN could be employed for segmenting cancer in 7 kinds of BTs. Primarily, this algorithm employed the feature extraction-based technique robust PCA to detect cancer position and mark in a database of Harvard Medical School.

Secondarily, a structure of the CNN technique was introduced for detecting BTs. Geetha and Gomathi [17] presented an approach named GW-DBN. Pre-processing was primarily implemented. During the segmentation method, the FCM technique was exploited. In the feature extraction technique, the GLCM and GRLM features have been removed. Besides, the study utilizes a DBN for classification. The enhanced DBN model has now been applied, and Grey Wolf Optimization (GWO) was employed.

## 3. The Proposed Model

In this article, an ABTDC-EODL technique was introduced for the detection and classification of the BT on brain MRI. The purpose of the ABTDC-EODL approach is to classify BT among adults as well as kids under the age of 10. To accomplish this, the ABTDC-EODL approach encompasses WF-based noise removal, ShuffleNet feature extractor, EO-based hyperparameter tuning, and SAE classification. Figure 1 describes the working flow of the ABTDC-EODL approach.

### 3.1. WF Based Pre-Processing

Primarily, the ABTDC-EODL method includes the WF technique to discard the noise that exists in it. The Wiener filter for image processing is a powerful mechanism used to improve the quality of images corrupted by different kinds of noise, namely Gaussian noise or motion blur [18].

It leverages the original image and the power spectral density of the noise to implement a weighted spatial-frequency domain filtering. The Wiener filter efficiently decreases noise while preserving essential image details by adaptively adjusting these weights, resulting in visually more transparent and more informative images.

### 3.2. ShuffleNet Feature Extractor

The ABTDC-EODL technique uses the ShuffleNet model to derive features. Researchers have developed a high-level performance and lightweight ShuffleNet network and convolutional neural network [19]. The author designed this to make use of Point Group Convolution (PGC) to enhance the

procedure effectiveness of convolution and then designed channel shuffle operation, which recognizes data interchange among dissimilar networks that aid in encrypting numerous information. When compared with numerous highly advanced network techniques, ShuffleNet decreases computational price and attains excellent performance while securing computational accuracy. As early as, Grouped Convolution (GC) is utilized in the AlexNet and some effective neural system models, namely Xception and MobileNet\_V2, which are designed advanced to lead depth-wise separate convolution on the baseline of GC.

However, the amount of computation and capacity of the technique can be organized; in this method, the computation of convolution absorbs a considerable quantity, and therefore, the Pixel-Level Group Convolution (PLGC) is specially developed inside the ShuffleNet model for decreasing Convolution Operation (CO). However, the CO can be limited to every GC only to decrease the computational complexity of the technique.

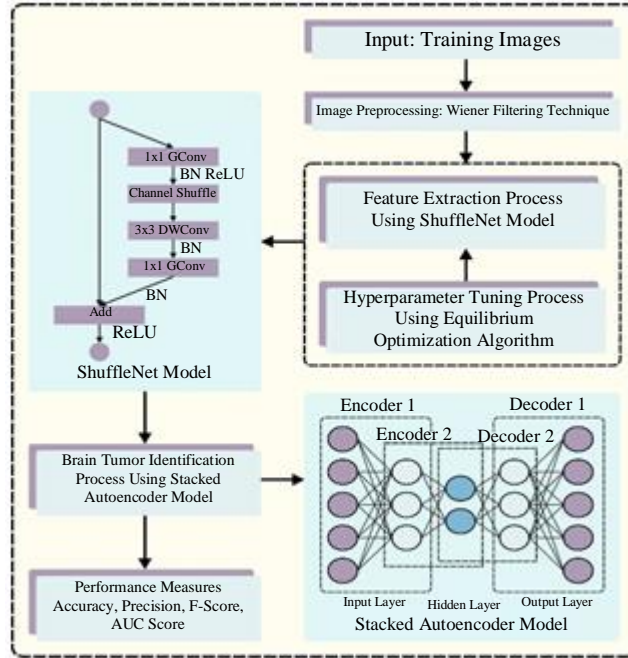


Fig. 1 Workflow of ABTDC-EODL approach

When many of the GCs are fixed, the feature detail of the outcome channels first comes from a small element of the input network wherever it is placed. Only the output is associated with the input inside the data, and a group of other groups cannot be achieved.

The input and output networks of ShuffleNet are established to a similar number for reducing memory consumption. For example, assume that the dimension of the feature maps is the number of input and output networks, and the convolution of height and width is.

As per to the Multiply Accumulate Operation (MAC) and Float Operations (FLOPs) calculation formula is given below:

$$B = h \cdot w \cdot (C_1 \times (1 \times 1) \times C_2) = h \cdot w \cdot C_1 \cdot C_2 \quad (1)$$

$$\begin{aligned} \text{MAC} &= h \cdot w \cdot C_1 + h \cdot w \cdot C_2 + (1 \times 1) \times C_1 \times C_2 \quad (2) \\ &= h \cdot w \cdot (C_1 + C_2) + C_1 \times C_2 \end{aligned}$$

With inequality,

$$(C_1 + C_2) \geq 2\sqrt{C_1 C_2} \quad (3)$$

Therefore,

$$MAC \geq 2\sqrt{hwB} + \frac{B}{h \cdot w} \quad (4)$$

In the formula mentioned above: where B is said to be FLOPs; the feature maps are w and h; Hence,  $C_1 = C_2$  i.e., when the input network remains equivalent to the output

channels, then the memory consumption is assumed to be small.

### 3.3. EO Based Parameter Tuning

In this work, the EO technique can be used for the parameter selection of the ShuffleNet model.

Particularly, based on the laws of physics, EO is used to balance the concentration of non-reactive constituents in a controlled volume [20].

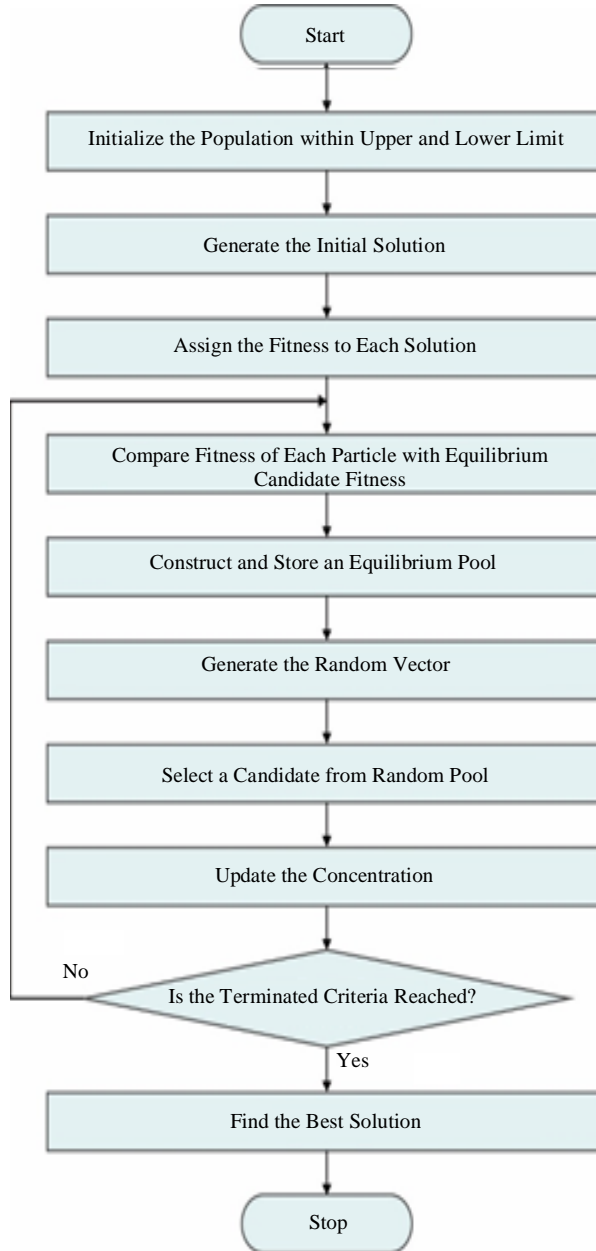


Fig. 2 Flowchart of EO

1) Initialization, 2) Equilibrium pool and candidates, and 3) Concentration update are the three mathematical stages of

EO discussed in the following. EO randomly produces a population like MA. The population comprises particles, and

a uniform distribution is attained as described by the concentration vector:

$$P_i^{\text{initial}} = P_{\min} + \text{rand}_i(P_{\max} - P_{\min}) \quad i = 1, 2, \dots, n \quad (5)$$

In Equation (5),  $P_{\max}$  and  $P_{\min}$  are the upper and lower boundaries, correspondingly,  $P_i^{\text{initial}}$  refers to the vector respective to the initial concentration of  $i^{\text{th}}$  particles,  $\text{rand}_i$  It is a random integer  $\in [0,1]$ , and  $n$  denotes the number of particles in the population:

$$\vec{P}_{\text{eq}} = [\vec{P}_{\text{eq}(1)}, \vec{P}_{\text{eq}(2)}, \vec{P}_{\text{eq}(3)}, \vec{P}_{\text{eq}(4)}, \vec{P}_{\text{eq}(\text{avg})}] \quad (6)$$

In every iteration, the EO is used to update the particle population by the subsequent equation:

$$\vec{P} = \vec{P}_{\text{eq}} + (\vec{P} - \vec{P}_{\text{eq}})\vec{F} + \frac{\vec{R}}{\lambda}(1 - \vec{F}) \quad (7)$$

In Equation (7),  $\vec{F}$  influences the exploration-exploitation balance:

$$\vec{F} = e^{-\lambda(t-t_0)} \quad (8)$$

In Equation (8),  $\lambda$  refers to the random integer  $\in [0, 1]$ , and the value of  $t$  reduces with increasing iteration number iter:

$$t = \left(1 - \frac{\text{iter}}{\text{Max\_iter}}\right)^{\left(a_2 \left(\frac{\text{iter}}{\text{Max\_iter}}\right)\right)} \quad (9)$$

In Equation (9), iter refers to the existing iteration and Max - iter denotes the maximal amount of iterations. The constant  $a_2$  used to control the exploitation. The vector  $\vec{t}_0$  is calculated by the following expression:

$$\vec{t}_0 = \frac{1}{\lambda} \ln \left( -a_1 \text{sign}(\vec{r} - 0.5) \left[ 1 - e^{-\lambda t} \right] \right) + t \quad (10)$$

Now the constant  $a_1$  used to control diversification. The term  $\text{sign}(r - 0.5)$  defines the diversification and intensification directions. The vector  $\vec{R}$  is represented as the generation rate and is calculated by Equation (11):

$$\vec{R} = \overline{\text{RCP}}(\vec{P}_{\text{eq}} - \vec{\lambda P})e^{-\lambda(t-t_0)} \quad (11)$$

Where,  $\overline{\text{RCP}}$  is :

$$\overline{\text{RCP}} = \begin{cases} 0.5r_1 & r_2 > \text{RP} \\ 0 & \text{otherwise} \end{cases} \quad (12)$$

Where  $r_1$  and  $r_2$  are random values  $\in [0,1]$  and parameter RP affects the exploitation-exploration balance. The fitness selection is a significant factor in the EO technique. An encoded solution is used to assess the goodness of the solution candidate. Here, the accuracy values are the most essential condition used to design an FF.

$$\text{Fitness} = \max(P) \quad (13)$$

$$P = \frac{\text{TP}}{\text{TP} + \text{FP}} \quad (14)$$

Where TP and FP characterize the true and the false positive values.

### 3.4. SAE Based Classification

For the classification process, the SAE model is used. An AE is a kind of FFNN where the input is similar to the output. The AE is used to compress the input into low-dimensional code and try to rebuild the outputs from these given representations [21]. As can be seen, the AE includes three different elements: the code, the encoder, and the decoder. The encoder compresses the input vector into hidden space to produce the code that the decoders can decode.

Precisely, using the decoder, the output is recreated from the code. Similar to AE, SAE is a stack of AE that learns in an unsupervised way. The bidirectional 2D-ConvLSTM architecture represents the SAE. The learning algorithm includes layer-by-layer-training to minimize the errors between inputs and outputs. The activation function used within the hidden unit is ReLU, whose mathematical expression can be given as follows:

$$g(z) = \max\{0, z\} \quad (15)$$

The HL of the prior one is the succeeding layer of AE, with each layer having an optimization function that is squared reconstructed error  $J$  of the single AE layer defined as follows:

$$\text{argmin}_{W_1, b_1, W_2, b_2} [J] = \text{argmin}_{W_1, b_1, W_2, b_2} \left[ \frac{\sum_{i=1}^m \|x_i - x'_i\| + J_{\text{wd}} + J_{\text{sp}}}{2} \right] \quad (16)$$

In Equation (16),  $x_i$  and  $x'_i$  are the  $i^{\text{th}}$  values of the input vector, along with its corresponding reconstruction version.  $J$  shows the squared reconstructed error of a single AE layer, and  $m$  is the size of the training dataset, respective to the size of the input time sequence.

## 4. Results and Discussion

In this section, the BT detection results of the ABTDC-EODL method are tested on the Br35H::Brain Tumour Detection 2020 dataset [22]. It comprises 3000 MRI samples with two classes, as represented in Table 1, and Figure 3 depicts the sample images.

Table 1. Details on database

Class	No. of Samples
Tumorous	1500
Non-Tumorous	1500
<b>Total Samples</b>	<b>3000</b>

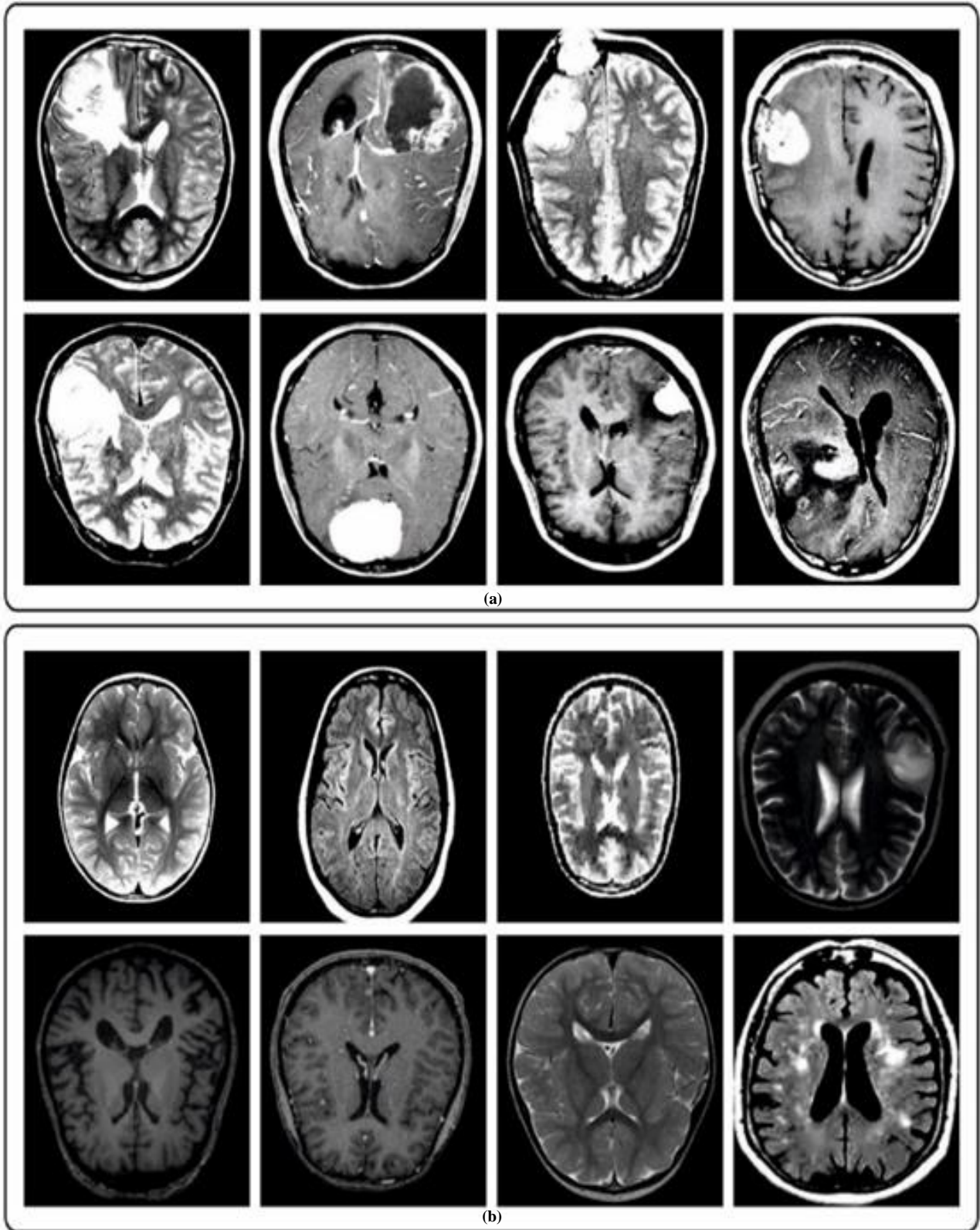


Fig. 3 Sample images

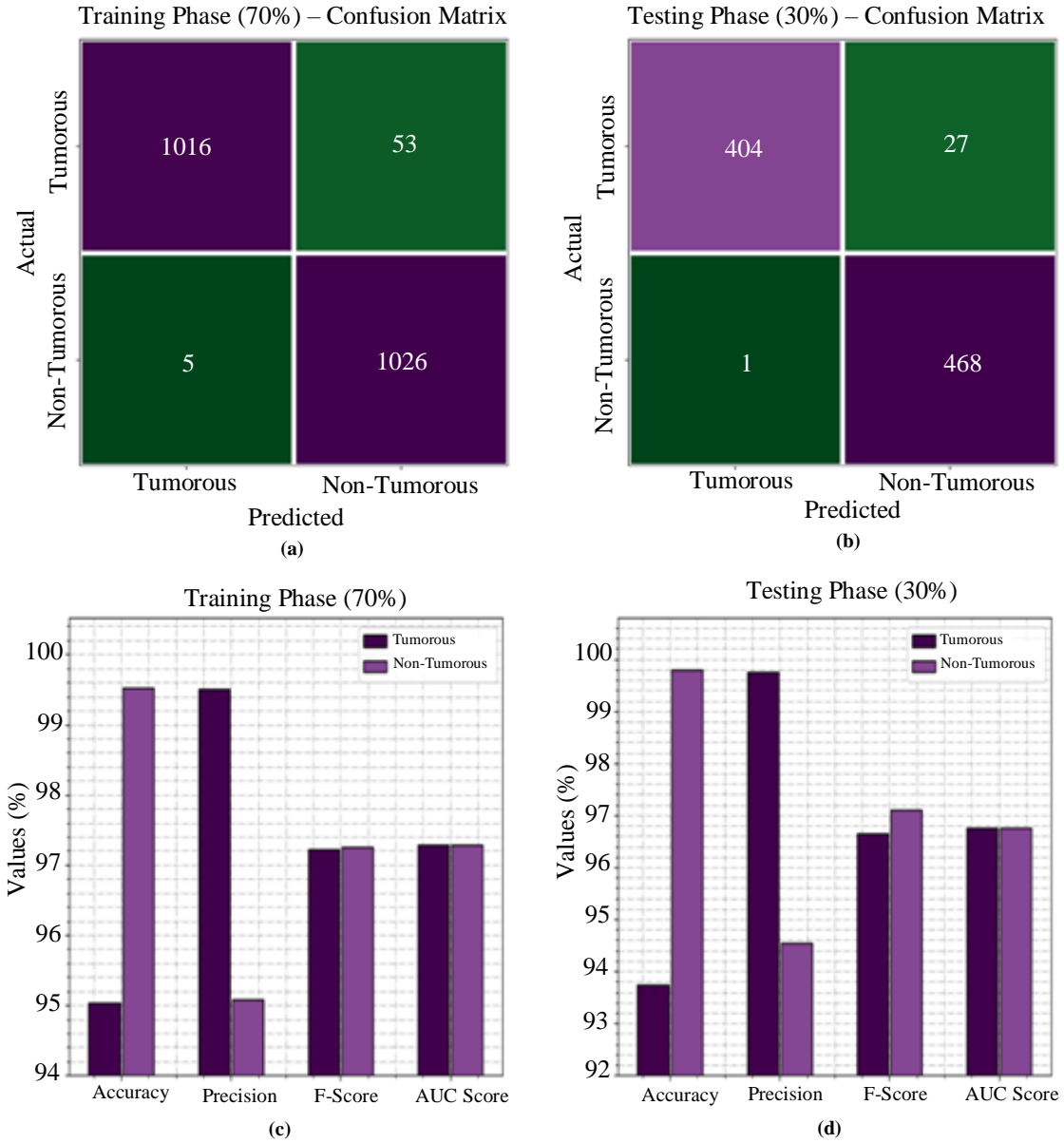


Fig. 4 (a-b) Confusion matrices, and (c-d) classifier outcome of 70:30 of TR phase/TS phase

Figure 4 defines the classifier performances of the ABTDC-EODL algorithm at 70:30 of the TR phase/TS phase. Figures 4(a)-4(b) demonstrates the confusion matrices achieved by the ABTDC-EODL approach.

The outcome value implied that the ABTDC-EODL methodology has classified and identified all two classes. Figures 4(c)-4(d) illustrates the classifier outcome of the ABTDC-EODL algorithm.

The outcomes stated that the ABTDC-EODL approach correctly classifies tumorous and non-tumorous images. In Table 2 and Figure 5, the BT detection results of the ABTDC-

EODL approach are clearly examined under 70:30 of the TR Phase/TS Phase. The results indicate that the ABTDC-EODL system properly categorizes Tumorous and non-tumorous images. Additionally, with 70% of the TR Phase, the ABTDC-EODL technique provides average accuracy, precision,  $F_{score}$  and  $AUC_{Score}$  values of 97.28%, 97.30%, 97.24%, and 97.28% respectively.

Also, with 20% of the TS Phase, the ABTDC-EODL model offers average accuracy, precision,  $F_{score}$  and  $AUC_{Score}$  values of 96.76%, 97.15%, 96.87%, and 96.76% correspondingly.

**Table 2. BT detection outcome of ABTDC-EODL approach on 70:30 of TR phase/TS phase**

Class	Accuracy	Precision	F <sub>score</sub>	AUC <sub>Score</sub>
<b>TR Phase (70%)</b>				
Tumorous	95.04	99.51	97.22	97.28
Non-Tumorous	99.52	95.09	97.25	97.28
<b>Average</b>	<b>97.28</b>	<b>97.30</b>	<b>97.24</b>	<b>97.28</b>
<b>TS Phase (30%)</b>				
Tumorous	93.74	99.75	96.65	96.76
Non-Tumorous	99.79	94.55	97.10	96.76
<b>Average</b>	<b>96.76</b>	<b>97.15</b>	<b>96.87</b>	<b>96.76</b>

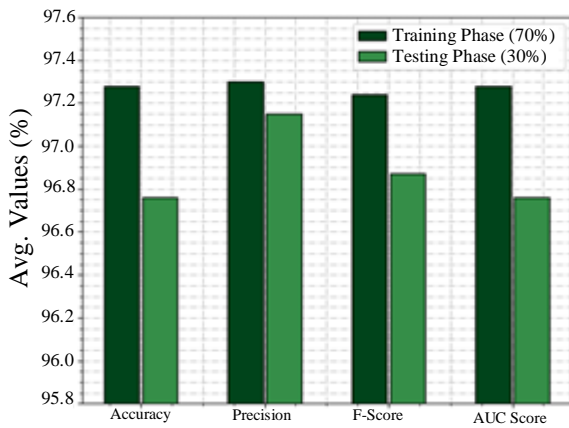


**Fig. 5 Average of ABTDC-EODL methodology on 70:30 of TR phase/TS phase**

To determine the performance of the ABTDC-EODL approach, TR and TS accuracy curves are described, as represented in Figure 6. The TR and TS accuracy curves signify the performance of the ABTDC-EODL system over various epochs.

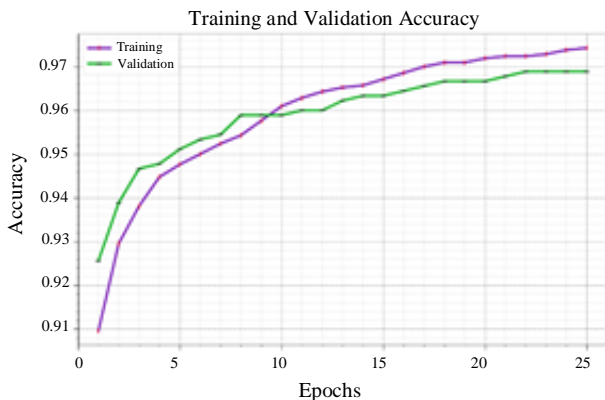
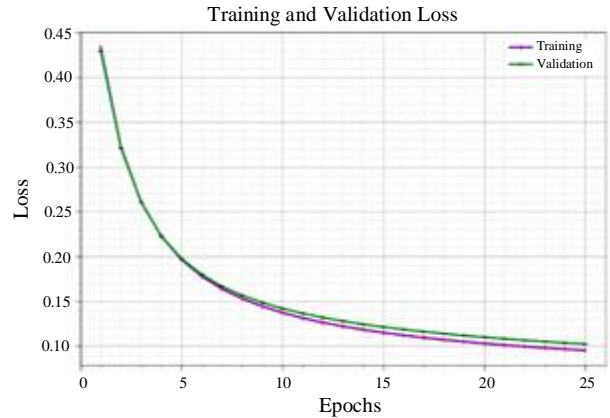


**Fig. 6 Accuracy curve of the ABTDC-EODL approach**

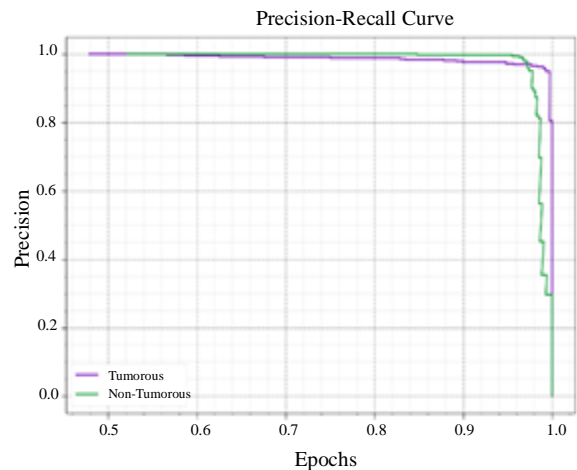
It is mentioned that the ABTDC-EODL technique achieves greater testing accuracy and has the potential to recognize the patterns in the TR and TS data.

Figure 7 illustrates the overall TR and TS loss values of the ABTDC-EODL approach over epochs. The TR loss indicates the model loss acquires reducing over epochs. Primarily, the loss values become diminished as the model adapts the weight to lessen the predictive error on the TR and TS data. The loss curves state the level where the model is fitting the training data.

It is observed that the TR and TS loss is gradually reduced and represents that the ABTDC-EODL system efficaciously learns the patterns identified in the TR and TS data. It is also established that the ABTDC-EODL model changes the parameters for minimizing the differentiation between the predicted and actual training labels. The PR curve of the ABTDC-EODL model is exhibited by plotting precision against recall, as represented in Figure 8. The outcome values indicate that the ABTDC-EODL technique gets raised precision-recall values under all two classes. The figure offers detailed information about the learning tasks and generalization abilities of the ABTDC-EODL algorithm. With an improvement in epoch count, it is evidenced that the TR and TS accu<sub>y</sub> curves get enhanced.



**Fig. 7 Loss curve of the ABTDC-EODL method**



**Fig. 8 PR curve of the ABTDC-EODL method**

The figure illustrates that the model learns to recognize different class labels. The ABTDC-EODL method achieves better results in the recognition of positive samples with reduced false positives. The ROC curves offered by the ABTDC-EODL system are demonstrated in Figure 9, which can differentiate the class labels. The figure specifies valuable insights into the trade-off between the TPR and FPR rates over various classification thresholds and differing counts of epochs. It provides the accurately predicted performance of the ABTDC-EODL approach on the classification of dissimilar classes.

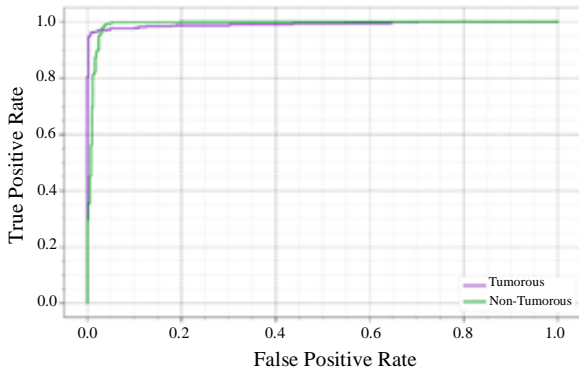


Fig. 9 ROC curve of the ABTDC-EODL approach

Table 3. Comparative outcome of ABTDC-EODL algorithm with existing systems

Model	Accuracy	Precision	F1Score
CNN Algorithm	96.56	94.81	94.94
3D CNN	96.49	94.17	94.58
CNN and NAND	96.00	94.49	94.56
Multi-scale CNN	97.00	95.80	96.07
DCNN	96.70	97.05	97.05
ABTDC-EODL	97.28	97.30	97.24

In Table 3 and Figure 10, a detailed comparison study of the ABTDC-EODL method is provided clearly [23]. The results indicate that the CNN, 3D CNN, CNN NAND, and DCNN models have shown worse results than other models with minimal classification performance. Along with that, the multi-scale CNN model has managed to obtain slightly improved results with accuracy of 97%, precision of 95.80%, and F1Score of 96.07%.

References

[1] B.J.D. Kalyani et al., “Analysis of MRI Brain Tumor Images Using Deep Learning Techniques,” *Soft Computing*, vol. 27, pp. 7535-7542, 2023. [CrossRef] [Google Scholar] [Publisher Link]

[2] Raheleh Hashemzahi et al., “Detection of Brain Tumors from MRI Images Base on Deep Learning Using Hybrid Model CNN and NADE,” *Biocybernetics and Biomedical Engineering*, vol. 40, no. 3, pp. 1225-1232, 2020. [CrossRef] [Google Scholar] [Publisher Link]

[3] D. Rammurthy, and P.K. Mahesh, “Whale Harris Hawks Optimization Based Deep Learning Classifier for Brain Tumor Detection Using MRI Images,” *Journal of King Saud University-Computer and Information Sciences*, vol. 34, no. 6, pp. 3259-3272, 2022. [CrossRef] [Google Scholar] [Publisher Link]

However, the ABTDC-EODL system exhibits superior performance with increased accuracy of 97.28%, precision of 97.30%, and F1Score of 97.24%. Thus, the ABTDC-EODL approach can be exploited for automated BT detection.

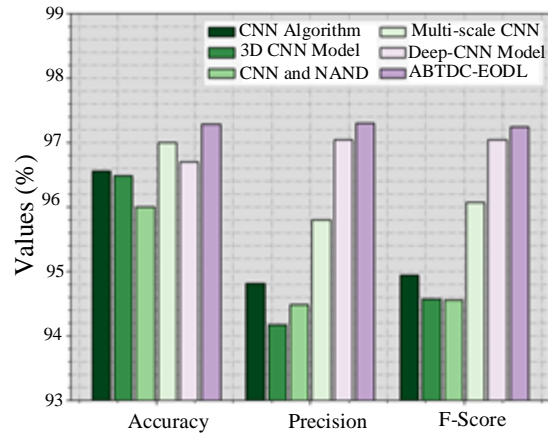


Fig. 10 Comparative outcome of ABTDC-EODL algorithm with existing systems

5. Conclusion

In this article, a novel ABTDC-EODL technique was introduced for the identification and classification of the BT on brain MRI. The purpose of the ABTDC-EODL approach is to classify BT among adults as well as kids under the age of 10.

To accomplish this, the ABTDC-EODL approach encompasses WF-based noise removal, ShuffleNet feature extractor, EO-based hyperparameter tuning, and SAE classification. Primarily, the ABTDC-EODL technique involves the WF technique to discard the noise that exists in it.

To derive features, the ABTDC-EODL technique uses the ShuffleNet model and its hyperparameters are selected by the EO algorithm. Finally, the SAE model was utilized to identify the presence of BT.

The ABTDC-EODL model can be validated on a benchmark Br35H: Brain Tumour Detection 2020 dataset, which encompasses 1500 Tumorous and 1500 non-Tumorous images. The obtained values highlight the better results of the ABTDC-EODL method over other existing techniques.

- [4] Akmalbek Bobomirzaevich Abdusalomov, Mukhriddin Mukhiddinov, and Taeg Keun Whangbo, "Brain Tumor Detection Based on Deep Learning Approaches and Magnetic Resonance Imaging," *Cancers*, vol. 15, no. 16, pp. 1-29, 2023. [[CrossRef](#)] [[Google Scholar](#)] [[Publisher Link](#)]
- [5] Md. Abu Bakr Siddique et al., "Deep Convolutional Neural Networks Model-Based Brain Tumor Detection in Brain MRI Images," *2020 Fourth International Conference on I-SMAC (IoT in Social, Mobile, Analytics and Cloud) (I-SMAC)*, Palladam, India, pp. 909-914, 2020. [[CrossRef](#)] [[Google Scholar](#)] [[Publisher Link](#)]
- [6] Saqib Ali et al., "A Comprehensive Survey on Brain Tumor Diagnosis Using Deep Learning and Emerging Hybrid Techniques with Multi-Modal MR Image," *Archives of Computational Methods in Engineering*, vol. 29, pp. 4871-4896, 2022. [[CrossRef](#)] [[Google Scholar](#)] [[Publisher Link](#)]
- [7] Arkapravo Chattopadhyay, and Mausumi Maitra, "MRI-Based Brain Tumour Image Detection Using CNN Based Deep Learning Method," *Neuroscience Informatics*, vol. 2, no. 4, 2022. [[CrossRef](#)] [[Google Scholar](#)] [[Publisher Link](#)]
- [8] Surendran Rajendran et al., "Automated Segmentation of Brain Tumor MRI Images Using Deep Learning," *IEEE Access*, vol. 11, pp. 64758-64768, 2023. [[CrossRef](#)] [[Google Scholar](#)] [[Publisher Link](#)]
- [9] Sneha Grampurohit et al., "Brain Tumor Detection Using Deep Learning Models," *2020 IEEE India Council International Subsections Conference (INDISCON)*, pp. 129-134, 2020. [[CrossRef](#)] [[Google Scholar](#)] [[Publisher Link](#)]
- [10] Driss Lamrani et al., "Brain Tumor Detection Using MRI Images and Convolutional Neural Network," *International Journal of Advanced Computer Science and Applications*, vol. 13, no. 7, pp. 452-460, 2022. [[CrossRef](#)] [[Google Scholar](#)] [[Publisher Link](#)]
- [11] T. Ruba, R. Tamilselvi, and M. Parisa Beham, "Brain Tumor Segmentation in Multimodal MRI Images Using Novel LSIS Operator and Deep Learning," *Journal of Ambient Intelligence and Humanized Computing*, vol. 14, pp. 13163-13177, 2023. [[CrossRef](#)] [[Google Scholar](#)] [[Publisher Link](#)]
- [12] Ebrahim Mohammed Senan et al., "Early Diagnosis of Brain Tumour MRI Images Using Hybrid Techniques between Deep and Machine Learning," *Computational and Mathematical Methods in Medicine*, vol. 2022, pp. 1-17, 2022. [[CrossRef](#)] [[Google Scholar](#)] [[Publisher Link](#)]
- [13] Mesut Togacar, Burhan Ergen, and Zafer Comert, "Brain MRNet: Brain Tumor Detection Using Magnetic Resonance Images with A Novel Convolutional Neural Network Model," *Medical Hypotheses*, vol. 134, 2020. [[CrossRef](#)] [[Google Scholar](#)] [[Publisher Link](#)]
- [14] Rahmeh Ibrahim, Rawan Ghnemat, and Qasem Abu Al-Haija, "Improving Alzheimer's Disease and Brain Tumor Detection Using Deep Learning with Particle Swarm Optimization," *AI*, vol. 4, no. 3, pp. 551-573, 2023. [[CrossRef](#)] [[Google Scholar](#)] [[Publisher Link](#)]
- [15] Muhammad Arif et al., "Brain Tumor Detection and Classification by MRI Using Biologically Inspired Orthogonal Wavelet Transform and Deep Learning Techniques," *Journal of Healthcare Engineering*, vol. 2022, pp. 1-19, 2022. [[CrossRef](#)] [[Google Scholar](#)] [[Publisher Link](#)]
- [16] Mohsen Ahmadi et al., "Detection of Brain Lesion Location in MRI Images Using Convolutional Neural Network and Robust PCA," *International Journal of Neuroscience*, vol. 133, no. 1, pp. 55-66, 2023. [[CrossRef](#)] [[Google Scholar](#)] [[Publisher Link](#)]
- [17] A. Geetha, and N. Gomathi, "A Robust Grey Wolf-Based Deep Learning for Brain Tumour Detection in MR Images," *Biomedical Engineering/Biomedical Technology*, vol. 65, no. 2, pp. 191-207, 2020. [[CrossRef](#)] [[Google Scholar](#)] [[Publisher Link](#)]
- [18] T. Kalaiselvi, T. Anitha, and Sriramakrishnan, "A Rician Noise Prediction and Removal Model for MRI Head Scans Using Wavelet Based Non-Local Median Filter," *Journal of Scientific Research of The Banaras Hindu University*, vol. 66, no. 5, pp. 75-87, 2022. [[CrossRef](#)] [[Google Scholar](#)] [[Publisher Link](#)]
- [19] Shih-Lin Lin, "Research on Tire Crack Detection Using Image Deep Learning Method," *Scientific Reports*, vol. 13, no. 1, pp. 1-17, 2023. [[CrossRef](#)] [[Google Scholar](#)] [[Publisher Link](#)]
- [20] Essam H. Houssein et al., "Development and Application of Equilibrium Optimizer for Optimal Power Flow Calculation of Power System," *Applied Intelligence*, vol. 53, no. 6, pp. 7232-7253, 2023. [[CrossRef](#)] [[Google Scholar](#)] [[Publisher Link](#)]
- [21] Aniekan Essien, and Cinzia Giannetti, "A Deep Learning Framework for Univariate Time Series Prediction Using Convolutional LSTM Stacked Autoencoders," *2019 IEEE International Symposium on Innovations in Intelligent Systems and Applications (INISTA)*, Sofia, Bulgaria, pp. 1-6, 2019. [[CrossRef](#)] [[Google Scholar](#)] [[Publisher Link](#)]
- [22] Br35H :: Brain Tumor Detection 2020. [Online]. Available: <https://www.kaggle.com/datasets/ahmedhamada0/brain-tumor-detection?select=no>
- [23] Dillip Ranjan Nayak et al., "Brain Tumor Classification Using Dense Efficient-Net," *Axioms*, vol. 11, no. 1, pp. 1-13, 2022. [[CrossRef](#)] [[Google Scholar](#)] [[Publisher Link](#)]